Original Article

DOI: 10.5582/bst.2019.01105

Protection of paeonol against epirubicin-induced hepatotoxicity: A metabolomic study

Xu Jing[1], Chao Sun[2], Huigang Chen[3], Jing Sun[2], Ying Zhang[2], Jing Wu[2,*]

[1] *Laboratory Medical Center, The Second Hospital of Shandong University, Ji'nan, China;*
[2] *Department of Pharmacy, The Second Hospital of Shandong University, Ji'nan, China;*
[3] *Department of Pathological Obstetrics, ZhuCheng Maternal and Child Health Hospital, Weifang, China.*

Summary **Paeonol extracted from the Moutan Cortex, possesses hepatoprotective activity against epirubicin (EPI)-induced liver damage. This study evaluated the protective effect of paeonol on EPI-induced hepatotoxicity and explored the underlying metabolomic mechanism. Breast tumor-bearing mice were randomly divided into three groups: control, EPI, and EPI + paeonol treatment. Mice received a tail *i.v.* injection of EPI every other day for 3 cycles or/and intragastrically (*i.g.*) administered paeonol daily for 6 days. Hematoxylin-eosin (HE) staining and biochemical detection were used to determine the degree of damage. A gas chromatography-mass spectrometry (GC-MS) technique was established to determine the metabolites. PLS-DA and PCA were used to investigate metabolic changes. HE staining and biochemical detection results showed that EPI caused serious liver damage while paeonol ameliorated it. The results of mass spectrogram, partial least squares-discriminate analysis (PLS-DA), and principal component analysis (PCA) demonstrated that lipid, amino acid, and energy metabolism involving seven metabolites were obviously changed by EPI and reversed by paeonol. Additionally, paeonol inhibited EPI-induced activation of adenosine monophosphate activated protein kinase/mammalian target of Rapamycin (AMPK/mTOR) signalling pathway. Our results demonstrated the hepatoprotective effect of paeonol on EPI-induced hepatotoxicity in mice, provided potential biomarkers for early assessment of EPI-induced liver injury and illuminated the metabolic mechanism underlying paeonol-related hepatic protection.**

Keywords: Paeonol, liver injury, GC-MS, metabolomic, AMPK/mTOR

1. Introduction

Epirubicin (EPI), an effective anthracycline antibiotic, is mainly metabolized in the liver, and its metabolites are associated with oxidative stress toxicity (*1*). EPI-induced liver toxicity is one of the major causes of hepatic dysfunction (*2*). Paeonol (2-hydroxy-4-methoxyacetophenone) is an active constituent isolated from the Chinese herbal medicine Moutan Cortex and Cynanchum paniculatum (*3*). Paeonol has been reported to have various biological activities, including anti-inflammatory, anti-allergic, and immune-regulation (*4*). In our previous studies, paeonol presented antioxidative stress activity, anti-inflammatory action, and apoptosis inhibition in EPI-induced liver damage by affecting the phosphatidylinositol 3-kinase/protein kinase B (PI3K/AKT) and nuclear factor (NF)-KB pathways (*5*).

EPI-induced hepatocyte oxidative stress and paeonol-related antioxidants change a series of biochemical parameters, which impact downstream metabolic processes (*6,7*). Conventional judgment of hepatotoxicity is principally according to the changes of aminopherases, including aspartate transaminase (AST), which increased after hepatonecrosis (*8*). Therefore, it is a priority to investigate potential indictors in initial liver injury induced by EPI and the treatment outcomes of paeonol.

With the development of analytical technologies, the metabolomic approach is widely used for the

Released online in J-STAGE as advance publication June 23, 2019.

*Address correspondence to:
Dr. Jing Wu, Department of Pharmacy, The Second Hospital of Shandong University, 247# Beiyuan Road, Ji'nan 250033, China.
E-mail: wujing19830603@126.com

identification of biomarkers for disease investigation and toxicity assessment (*2*). The combined application of mass spectrometry and chromatography is gaining widespread use in metabolomic studies, and the most common technique is gas chromatography-mass spectrometry (GC-MS) for its strategic advantages (*9*). In the present work, GC-MS-based pairwise comparative metabolomic was applied to investigate the altered metabolites in serum and uncover the potential metabolic processes following EPI and paeonol treatment. The results demonstrate potential biomarkers for early assessment of EPI-induced hepatotoxicity and illuminate the metabolic mechanism underlying paeonol-related hepatic protection.

2. Materials and Methods

2.1. *Materials*

EPI and paeonol (purity, 99.12% by high-performance liquid chromatography: HPLC) were purchased from Sigma-Aldrich, Inc., St. Louis, MO, USA. Trimethyl-chlorosilane (TMCS) and n-heptadecanoic acid was purchased from Sinopharm Chemical Reagent Co., Ltd. (Shanghai, China). Methoxy pyridine was purchased from Tianjin Kermel Chemical Reagent Co., Ltd. (China). HPLC grade acetonitrile and n-hexane were purchased from J.T. Baker (USA).

2.2. *Instruments*

Agilent 7890A-5975C GC-MS (Agilent Technologies, Inc., USA), XW-80A vortex mixers (Jingke Industrial Co., Ltd., Shanghai, China), MS205 DU electronic scale (Metteler-Toledo, Shanghai, China), ABBOTT centrifuge (Abbott Laboratories, USA) and KD-500DE ultrasound cleaner (Kunshan Ultrasonic Instrument Co., Ltd., China) were used.

2.3. *Animals*

Female BALB/c mice (aged 6-8 weeks, weighing 18-22 g) were purchased from the Laboratory Animal Centre, of Shandong University in China. The animals were housed under specific-pathogen free conditions at the Animal Centre of the Department of Pharmacology of the School of Medicine of Shandong University in China. The protocol for the *in vivo* study with mice conforms to the Guide for the Care and Use of Laboratory Animals published by the US National (Permit Number: KYLL-2017(GJ)A-0028). All experiments were approved by the Ethics Committee of The Second Affiliated Hospital of Shandong University.

2.4. *Experimental design*

A breast tumor-bearing mice model was established as previously described (*8*). In brief, BALB/c mice were subcutaneously injected with 4T1 cells (suspension, 100 μL, 5×10^6 cells/mL) in the right side of the fourth mammary gland. The tumor length and width were measured using a digital caliper, and the tumor volume was calculated using the following formula: tumor volume (mm^3) = (length × $width^2$)/2. When the size of the tumors was approximately 100 mm^3, the mice were randomly divided into three groups: control, EPI, and EPI + paeonol treatment:

Control group: mice received intragastrically (*i.g.*) administered saline daily for 6 days and a tail intravenous (*i.v.*) injection of saline every other day for three cycles;

EPI group: mice received *i.g.* saline daily for 6 days and a tail *i.v.* injection of EPI (6 mg/kg) every other day for 3 cycles;

Combined group: mice received *i.g.* paeonol (30 mg/kg) daily for 6 days and a tail *i.v.* injection of EPI (6 mg/kg) every other day for 3 cycles.

Blood was collected and the mice were sacrificed on day 8. The liver tissues were removed rapidly. Some livers were fixed in formalin for hematoxylin and eosin (HE) staining, whereas others were frozen in liquid nitrogen (stored at -80°C) for Western blot analysis.

2.5. *Histopathological examination and assay of hepatic marker enzymes*

Liver tissues were fixed in 10% buffered formalin, embedded in paraffin, sectioned (5 mm thick) and stained with HE for histopathological analysis under light microscope (CKX41, 170 Olympus, Tokyo, Japan). Samples were obtained after centrifugation (4,000 rpm, 5 min) to monitor the biochemistry index. The alanine aminotransferase (ALT), glutamic-oxalacetic transaminease (AST) and alkaline phosphatase (ALP) in plasma were assayed according to the manufacturer's instructions (Nanjing Jiancheng Biotechnology Institute, China).

2.6. *Western blot analyses*

Western blots were analyzed as described previously (*8*). All procedures followed the suppliers' instructions. Livers were cut into small pieces, homogenized in pyrolysis liquid (containing phenylmethylsulfonyl fluoride) on ice and centrifuged at 12,500 rpm for 5 min at 4°C. Supernatants were harvested to denature by boiling for 5 min in loading buffer.

Samples were electrophoresed, electro-transferred onto polyvinylidene difluoride (PVDF) membranes, incubated with primary antibodies and secondary antibodies, visualised using chemiluminescence reagent (Millipore, USA) and exposed to X-ray film. Data was quantitated by comparison to vehicle control using Image Jet software. Triplicate experiments with

triplicate samples were conducted. Primary antibodies were all from Cell Signalling Technology (Beverly, MA), including p-AMPK (adenosine monophosphate activated protein kinase, 1:900), AMPK (1:1000), p-mTOR(mammalian target of Rapamycin, 1:800), mTOR (1:1000), LC3(1:1000), Atg5(1:1000), Atg7(1:1000), Beclin1(1:1000) and β-actin (1:1000).

2.7. *Blood sample preparation*

Blood samples were collected and centrifuged for 5 min at 4,000 rpm. Plasma was separated and stored at -80°C until analysis. Acetonitrile (250 μL) was added to 100 μL of serum (ice-bath for 15 min), vortexed for 3 min, then centrifuged at 10,000 rpm for 10 min. The supernatant (150 μL) was transferred to a GC vial and evaporated under a stream of nitrogen gas to dryness. Fifty μL of methoxypyridine (15 mg/mL) was added to the vial for 1 h at 70°C, and 50 μL of derivatization reagent (N-methyl-N (trimethylsily) trifluoroacetamide : trimethylchlorosilane = 100:1, V/V) was then added. The combined solution was kept at 70°C for another hour, vortexed after adding 150 μL n-hexane (0.10 mg/mL of heptadecanoic acid) as an internal standard and centrifuged to separation (3,000 rpm for 10 min). The liquid supernatant was drawn for GC-MS analysis (*10*).

2.8. *GC-MS analysis*

The derivative sample (2 μL) was injected into GC-MS. An HP-5MS column (0.25 mm × 30 m × 0.25 mm, Agilent, USA) was used in metabolite studies, and the helium carrier gas pressure was set at 10 psi. The GC oven was initially set at 85°C for 1 min, increased to 180°C at a rate of 10°C/mL and then kept at 260°C for 15 min. MS detection was conducted in EI mode with an electron energy of 70 eV and full scan mode with m/z of 60 to 600, followed by splitless mode injection (*10*).

2.9. *Metabolomic analysis*

MSD Chemstation software (Version E02.00.493, Agilent Technologies) was used to process the GC-MS data. Endogenous metabolites were identified by matching the spectra against the reference library of NIST 08 Identification System. The metabolite data derived from the three groups were further analyzed using pattern recognition methods in software SIMCA-P+ 11.5 (UmetricsAB, Umea, Sweden). The dataset was subjected to normalization and pare to scaling prior to multivariate analysis. Partial least squares-discriminate analysis (PLS-DA) and principal component analysis (PCA) were used to explain the maximum variation and separation among the defined class samples. Variable importance in the projection (VIP) was used to interpret the specific metabolites among classes. Sixteen concentrations of potential biomarkers in the control, EPI, and EPI + paeonol groups were introduced into SPSS/Win 11.0 software (SPSS Inc., Chicago, IL) for further *t*-tests, and a p value of < 0.05 or $< 0.01$was considered statistically significant ($^{*}p < 0.05$,$^{\#}p < 0.01$) (*10,11*).

3. Results

3.1. *Changes of histopathology and biomarkers*

4T1-tumor bearing mice were treated three times with EPI at 6 mg/kg, a cumulative dose that can cause hepatotoxicity in mice (*5*). In our present study, histopathology of HE staining from control mice livers showed normal architecture. HE-stained liver sections (Figure 1A) from mice treated with EPI had severe liver damage characterized by infiltration of inflammatory cells, interstitial hemorrhage and necrosis. However, samples from the combined group represented histopathological changes in mitigation compared to those receiving EPI alone.

The ALT, AST and ALP activities in plasma, the most widely adopted drug-induced liver injury biomarkers for hepatotoxicity, were measured to evaluate EPI-induced liver damage. Samples in EPI-treated mice demonstrated increased levels of ALT, AST and ALP. By contrast, the combination of EPI and paeonol resulted in an apparent reversal of the EPI-induced increase in liver function enzymes (Figure 1B).

3.2. *Analysis of metabolite profiling*

GC-MS analysis was performed to separate the complex endogenous metabolites. The typical total ion chromatography (TIC) of three groups of samples is displayed in Figure 2. Based on the metabolic profile data, more than 50 metabolites were detected in the plasma. After derivatization, normalization and filtering steps, 16 metabolites with a degree of matching above 80% were selected and identified by calculating on the basis of confirmed ion and fragmentation patterns and compared with the mass spectrum of the library, as shown in Table 1. The relative standard deviation (RSD) of each common peak was less than 15% ($n = 5$), showing that the precision of analytical platforms was excellent.

GC-MS results suggested that the metabolite spectrum in the plasma mainly included contributions from amino acids and lipids, which are probably associated with oxidative stress induced by EPI. The concentrations of the substances inside the body are related to the energy metabolism and autophagy activity.

3.3. *Multivariate statistical analysis*

To illustrate the differences in metabolic profiles, the

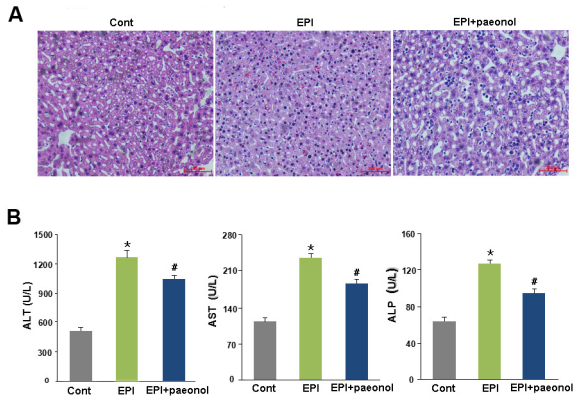

Figure 1. Effects of paeonol on EPI-induced hepatic dysfunction. Mice were treated with saline, EPI (6 mg/kg) every other day for 3 cycles and/or paeonol (30 mg/kg) daily for 6 days. Then, electrocardiographs **(A)** and myocardial enzymes **(B)** were examined, and the data were statistically significant (mean ± S.E.M.; *$p < 0.05$ versus control, #$p < 0.05$ versus EPI-treated mice).

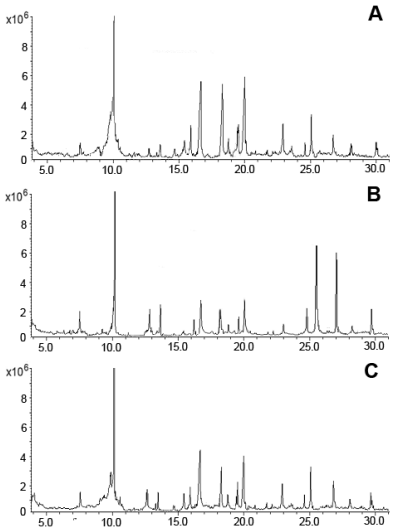

Figure 2. The typical total ion current chromatograms (TIC) of three samples. The TIC of **(A)** control samples, **(B)** EPI group and **(C)** EPI+paeonol group by GC-MS analysis.

Table 1. Summary of the changes in relative levels of metabolites in mice plasma indicated by the PLS-DA loading plots and statistical analysis

No.	Metabolites compounds	Retention time/min	EPI *vs*. CONT	EPI+PAE *vs*. EPI
1	Lactic acid	7.51	↑	↓
2	L-Alanine	12.85	↓	↑
3	Glycine	15.92	↓#	↑#
4	L- Serine	16.49	↑#	↓#
5	L-Valine	13.28	↑*	↓*
6	L- Leucine	15.37	↑*	↓*
7	L- Threonine	18.26	↓	↑
8	L-Aspartic acid	18.93	↓	↑
9	Palmitic acid	19.50	↓#	↑#
10	Oleic acid	20.83	↓#	↑#
11	Galactose	22.95	↓	↑
12	Succinic acid	24.63	↑#	↓#
13	Malic acid	25.14	↑*	↓*
14	Citric acid	26.87	↑	↓
15	Stearic acid	28.14	↓	↑
16	Cholesterol	30.02	↑	↓

Marks indicate the direction of the change, *i.e.*, ↓ for decrease, ↑ for increase; #$p < 0.05$ and *$p < 0.01$, as indicated by the statistical analysis *t*-test.

GC-MS spectra were further segmented and subjected to PCA. The score plot clearly discriminated the distinct separation of the three groups: control, EPI, and EPI + paeonol (Figure 3). The control group was clustered to the under-right section, while EPI-treated groups generally clustered in the opposite region. The combined group was located between the control and EPI-treated groups.

PLS-DA was performed to further identify the metabolites underlying the differences among the groups. As shown in Figure 4, the score plots show a complete separation between the control and EPI-treated groups, in which the control group clustered to the right, while locations of the EPI-treated group generally moved to the lower-left region. The combined group moved away from the EPI-treated group, tending to move toward the controls. The results implied that the overall metabolism of the EPI-treated mice changed significantly, and the metabolites in co-treated mice represented a tendency to move closer to the controls. In addition, the outliers in the groups were probably caused by individual differences.

On the basis of the cross-validated PLS-DA model and *t*-test analysis, the VIP was calculated. Seven endogenous metabolites whose VIP values were larger than 1 were selected as the candidates of the potential biomarkers for EPI-induced liver injury. Serum levels of glycine and oleic acid were lower in the EPI group than those in the controls, while amounts of malic acid, L-leucine, L-valine, succinic acid and serine were higher. The coefficient column plot of the latent variables using PLS-DA is shown in Figure 5.

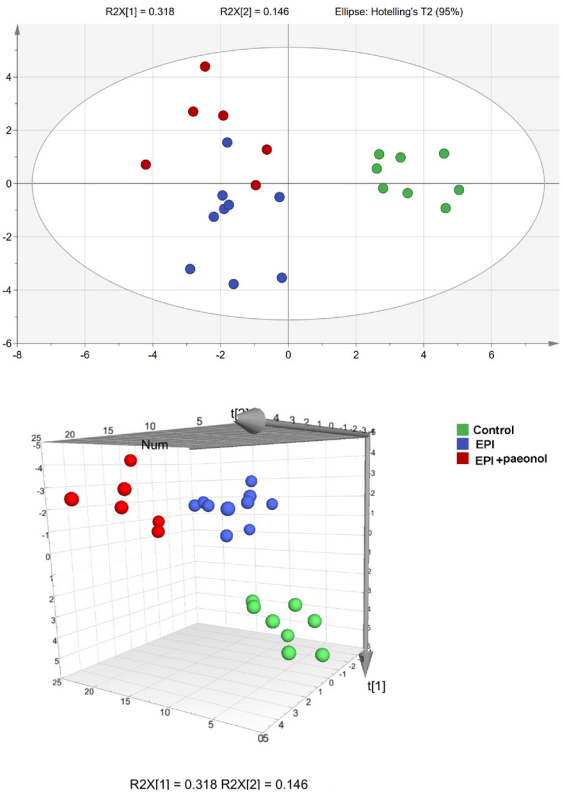

Figure 3. The PCA statistical analysis results. The PCA scores plot mapping GC-MS spectra of control, EPI, and EPI+paeonol groups.

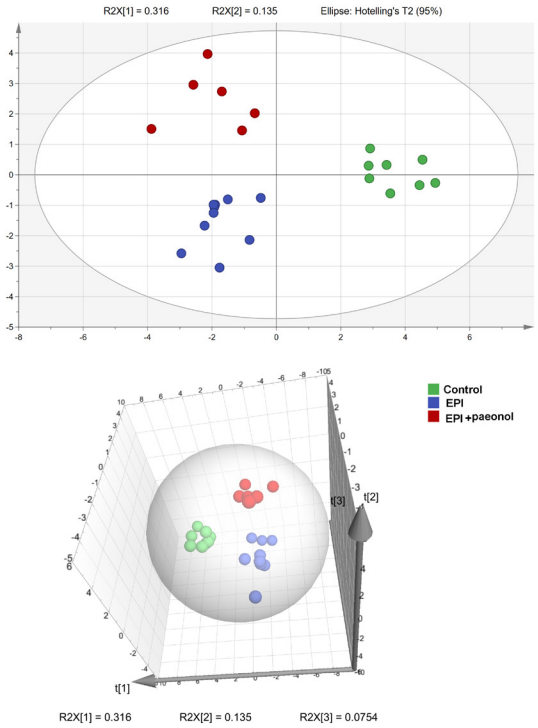

Figure 4. The PLS-DA statistical analysis results. The PLS-DA scores plot mapping GC-MS spectra of control, EPI, and EPI+paeonol groups.

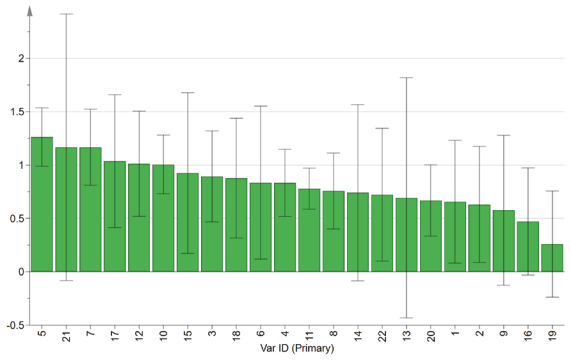

Figure 5. The VIP statistical analysis results. The VIP was calculated on the basis of the cross-validated PLS-DA model and t-test analysis.

3.4. *Relative signalling pathway*

To verify that the protective effect against EPI-induced hepatotoxicity afforded by paeonol requires autophagy inhibition. The efficiency of the autophagy was confirmed by Western blot analysis. As shown in Figure 6, the EPI treatment significantly reduced p-mTOR level, and increased p-AMPK, LC3II/LC3I, Atg5, Atg7, Beclin1 levels in livers. We next exposed EPI-treated and then subjected them to scrambled or paeonol. The results showed that paeonol significantly attenuated the autophagy activation, the protective effects of paeonol, indicating paeonol-dependent protection against EPI-induced autophagy activation in liver.

4. Discussion

EPI is an effective anthracycline antibiotic that is widely used to treat various malignancies. Nevertheless, EPI-induced liver injury is a concern depending on the dosage and duration of therapy, resulting in hepatic dysfunction and acute liver failure. EPI has been shown to be metabolized by the liver, and its metabolites are related to oxygen-free radicals, which lead to liver toxicity (*1*). In our previous research, EPI was able to activate the PI3K/Akt/NF-kB pathway to enhance oxidative stress and induce hepatocyte apoptosis in 4T1-tumor mice. Despite much research, the precise mechanism underlying the EPI-induced acute and chronic normal liver tissue damage should be further explored.

In the current study, we observed that the serum ALT, AST and ALP, as well as HE staining confirmed EPI-induced liver damage and paeonol-related hepatoprotective effects, which are consistent with published literature (*12*). In addition, a metabolomic analysis of systemic variation following EPI and paeonol treatment was also investigated in mice. The metabolic markers of EPI and paeonol were distinguishable in a well-established plasma GC-MS-based metabolomic profile. A panel of candidate endogenous metabolites was identified as potential biomarkers.

The results indicated that the metabolic alteration,

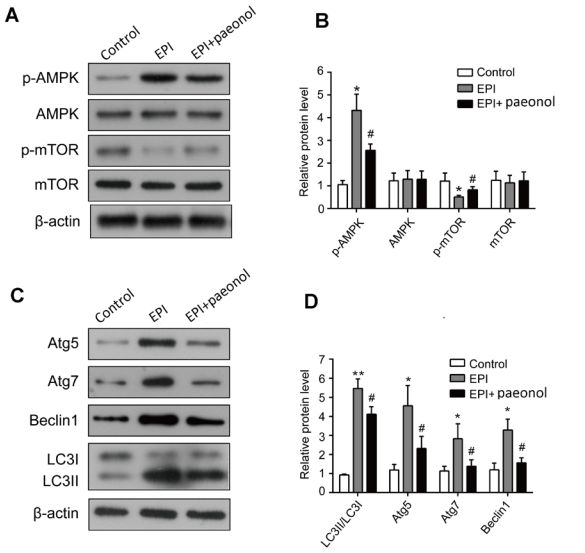

Figure 6. Paeonol mitigates the EPI-induced hepatotoxicity via the AMPK/mTOR pathway. (A) The expression levels of p-AMPK, AMPK, p-mTOR and mTOR in livers were inspected by Western blotting. **(B)** Data were quantitated to represent mean ± S.E.M. ($n \geq 3$). **(C)** The expression levels of LC3II/LC3I, Atg5, Atg7 and Beclin1 in livers were inspected by Western blotting. **(D)** Data were quantitated to represent mean ± S.E.M. ($n \geq 3$). (*$p < 0.05$ versus control, #$p < 0.05$ versus EPI-treated mice).

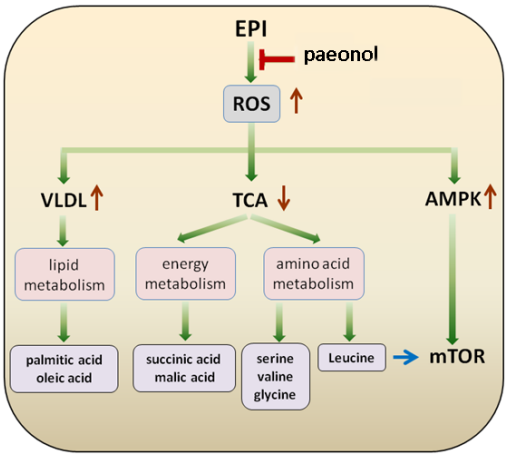

Figure 7. The possible molecular mechanism of the hepatoprotective effect of paeonol on EPI-induced hepatotoxicity in mice.

including increments of 5 metabolites in plasma, and decrements of 2 metabolites in plasma occurred after EPI treatment. It is noteworthy that all metabolite alteration could be reversed by paeonol treatment, suggesting possible pharmacological mechanisms of the hepatoprotective effect of paeonol. The changed metabolites related to some potential metabolic pathways: lipid metabolism (palmitic acid and oleic acid), amino acid metabolism (serine, valine, leucine, and glycine) and energy metabolism (succinic acid and malic acid).

Our previous study demonstrated that the generation of reactive oxygen species (ROS) is one of the major proposed mechanisms of EPI-induced liver injury, which leads to cell membrane damage and results in the release of marker enzymes of hepatotoxicity. Under the condition of oxidative stress, the tricarboxylic acid (TCA) cycle is slowed down, resulting in decreased production of ROS (*13,14*). The two crucial energy supply substances for the mitochondrial TCA cycle, succinic acid and malic acid are increased due to the dysfunction of mitochondria (*15*). Furthermore, gluconeogenesis is also inhibited under oxidative stress, resulting in an increase of serine, which is able to synthesize hepatic glucose (*16*). In addition, the synthesis of very low-density lipoproteins (VLDL) is significantly affected in transporting lipids from liver to plasma by dysfunction of hepatic enzymes, contributing to a decrease of palmitic acid and oleic acid (*17*). Furthermore, a mass of ROS leads to the consumption of antioxidants, such as glutathione (GSH), which is synthesized with glycine, glutamate and cysteine in the liver (*18*). Therefore, the decrease of glycine in the EPI-treated group is closely associated with the large amount of GSH synthesis. We previously found that paeonol was able to exert its anti-oxidative stress activity in EPI-induced hepatotoxicity (*8*). In our present study, compared to EPI-treatment, succinic acid, malic acid and serine are reduced and palmitic acid, oleic acid and glycine are elevated in the paeonol-treated group.

The branched-chain amino acids (BCAAs), including valine, leucine, and isoleucine, have been reported in liver, renal and other tissue injuries (*19,20*). Holeček *et al*. observed that the BCAAs are extremely decreased both in carbon tetrachloride and ischaemic acute liver damage. As essential amino acids, valine and leucine not only participate in protein metabolism, but also have various physiological and metabolic functions (*21*). After being converted into α-ketoisovalerate (KIV, ketovaline) and α-ketoisocaproate (KIC, ketoleucine), valine and leucine can be oxidized by the liver and then be catabolized to succinyl-CoA and acetyl-CoA, which enter into the TCA cycle (*22*). The elevation of BCAA levels may result from amino acids leaking from the dying hepatocytes into the circulatory system (*19*). In our study, valine and leucine increased dramatically in the EPI group compared to the controls.

The AMP-activated protein kinase (AMPK) is a central regulator of cellular and organismal metabolism (*23*). In eukaryotes, AMPK plays a crucial role in metabolism, especially in energy homeostasis in the liver and other dedicated tissues (*24,25*). It is activated when ATP production is lower, resulting in a relatively increased AMP/ATP ratio (*26*). The activation of AMPK can suppress the mTOR pathway by directly phosphorylating raptor (*15*). In addition, leucine was shown to enhance AMPK activity to promote palmitate uptake both *in vitro* and *in vivo* (*27*). On the other hand, leucine has been shown to function as a regulator to activate the mTOR signalling pathway, involved in the stimulation of protein synthesis (*28*). In our study, we

found that the expression of p-AMPK is augmented, and p-mTOR is distinctly decreased in EPI treatment compared to the controls. Furthermore, the activation of AMPK inducing the inhibition of mTOR-dependent signalling may be expected to stimulate autophagy. Figure 7 shows the possible molecular mechanism of the hepatoprotective effect of paeonol on EPI-induced hepatotoxicity. Therefore, whether the autophagy level is changed in EPI-induced hepatotoxicity should be studied further in future research.

In conclusion, our results demonstrate the hepatoprotective effect of paeonol on EPI-induced hepatotoxicity in mice. The underlying metabolomic mechanisms refer to lipid metabolism (palmitic acid and oleic acid), amino acid metabolism (serine, valine, leucine and glycine), energy metabolism (succinic acid and malic acid) and the AMPK/mTOR signalling pathway. Our study is not only beneficial to the understanding of the pathogenetic mechanism of EPI-induced hepatotoxicity, but also provides experimental data and a theoretical foundation for the hepatoprotective effect of paeonol.

Acknowledgements

This work was supported by Shandong Key Research and Development Program (2018GSF118075), National Natural Science Foundation of China (81703617), National Natural Science Foundation of China (81801163).

References

1. Weenen H, van Maanen JM, de Planque MM, McVie JG, Pinedo HM. Metabolism of 4'-modified analogs of doxorubicin. unique glucuronidation pathway for 4'-epidoxorubicin. Eur J Cancer Clin Oncol. 1984; 20:919-926.
2. Henninger C, Huelsenbeck J, Huelsenbeck S, Grosch S, Schad A, Lackner KJ, Kaina B, Fritz G. The lipid lowering drug lovastatin protects against doxorubicin-induced hepatotoxicity. Toxicol Appl Pharmacol. 2012; 261:66-73.
3. Lee H, Lee G, Kim H, Bae H. Paeonol, a major compound of moutan cortex, attenuates Cisplatin-induced nephrotoxicity in mice. Evid Based Complement Alternat Med. 2013; 2013:310989.
4. Li H, Wang SW, Zhang BL. Pharmacological action and pharmacokinetics of paeonol. Asia-Pacific Tradit. Med. 2010b; 6:110-112.
5. Wu J, Xue X, Zhang B, Jiang W, Cao H, Wang R, Sun D, Guo R. The protective effects of paeonol against epirubicin-induced hepatotoxicity in 4T1-tumor bearing mice *via* inhibition of the PI3K/Akt/NF-kB pathway. Chem Biol Interact. 2016; 244:1-8.
6. Sun Z, Du J, Hwang E, Yi TH. Paeonol extracted from Paeonia suffruticosa Andr. ameliorated UVB-induced skin photoaging *via* DLD/Nrf2/ARE and MAPK/AP-1 pathway. Phytother Res. 2018; 32:1741-1749.
7. Zhang A, Sun H, Wang X. Serum metabolomics as a novel diagnostic approach for disease: a systematic review. Anal Bioanal Chem. 2012; 404:1239-1245.
8. Wu J, Xue X, Zhang B, Cao H, Kong F, Jiang W, Li J, Sun D, Guo R. Enhanced antitumor activity and attenuated cardiotoxicity of Epirubicin combined with Paeonol against breast cancer. Tumour Biol. 2016; 37:12301-12313.
9. Deng M, Zhang M, Sun F, Ma J, Hu L, Yang X, Lin G, Wang X. A gas chromatography-mass spectrometry based study on urine metabolomics in rats chronically poisoned with hydrogen sulfide. Biomed Res Int. 2015; 2015:295241.
10. Wei C, Li Y, Yao H, Liu H, Zhang X, Guo R. A metabonomics study of epilepsy in patients using gas chromatography coupled with mass spectrometry. Mol Biosyst. 2012; 8:2197-2204.
11. Lu X, Zhao Q, Tian Y, Xiao S, Jin T, Fan X. A metabonomic characterization of (+)-usnic acid-induced liver injury by gas chromatography-mass spectrometry-based metabolic profiling of the plasma and liver in rat. Int J Toxicol. 2011; 30:478-491.
12. Wu J, Xue X, Zhang B, Jiang W, Cao H, Wang R, Sun D, Guo R. The protective effects of paeonol against epirubicin-induced hepatotoxicity in 4T1-tumor bearing mice *via* inhibition of the PI3K/Akt/NF-kB pathway. Chem Biol Interact. 2016; 244:1-8.
13. Liu J, Litt L, Segal MR, Kelly MJ, Pelton JG, Kim M. Metabolomics of oxidative stress in recent studies of endogenous and exogenously administered intermediate metabolites. Int J Mol Sci. 2011; 12:6469-6501.
14. OuYang Q, Tao N, Zhang M. A damaged oxidative phosphorylation mechanism is involved in the antifungal activity of citral against penicillium digitatum. Front Microbiol. 2018; 9:239.
15. Shin DJ, Kim JE, Lim TG, Jeong EH, Park G, Kang NJ, Park JS, Yeom MH, Oh DK, Bode AM, Dong Z, Lee HJ, Lee KW. 20-*O*-beta-D-glucopyranosyl-20(S)-protopanaxadiol suppresses UV-Induced MMP-1 expression through AMPK-mediated mTOR inhibition as a downstream of the PKA-LKB1 pathway. J Cell Biochem. 2014; 115:1702-1711.
16. Huang X, Shao L, Gong Y, Mao Y, Liu C, Qu H, Cheng Y. A metabonomic characterization of CCl4-induced acute liver failure using partial least square regression based on the GC/MS metabolic profiles of plasma in mice. J Chromatogr B Analyt Technol Biomed Life Sci. 2008; 870:178-185.
17. Martin P. The oxford textbook of clinical hepatology. Gastroenterology. 2000; 118:449.
18. Abeti R, Baccaro A, Esteras N, Giunti P. Novel Nrf2-inducer prevents mitochondrial defects and oxidative stress in Friedreich's Ataxia models. Front Cell Neurosci. 2018; 12:188.
19. Holecek M, Mráz J, Tilšer I. Plasma amino acids in four models of experimental liver injury in rats.Amino Acids. 1996;10:229-241.
20. Teplan V, Schuck O, Horackova M, Skibova J, Holecek M. Effect of a keto acid-amino acid supplement on the metabolism and renal elimination of branched-chain amino acids in patients with chronic renal insufficiency on a low protein diet. Wien Klin Wochenschr. 2000; 112:876-881.
21. Bifari F, Nisoli E. Branched-chain amino acids differently modulate catabolic and anabolic states in mammals: A pharmacological point of view. Br J Pharmacol. 2017;

174:1366-1377.
22. Holecek M. Branched-chain amino acids in health and disease: Metabolism, alterations in blood plasma, and as supplements. Nutr Metab (Lond). 2018; 15:33.
23. Hardie DG. AMP-activated protein kinase: An energy sensor that regulates all aspects of cell function. Genes Dev. 2011; 25:1895-1908.
24. Hardie DG, Ross FA, Hawley SA. AMPK: A nutrient and energy sensor that maintains energy homeostasis. Nat Rev Mol Cell Biol. 2012; 13:251-262.
25. Ki SH, Choi JH, Kim CW, Kim SG. Combined metadoxine and garlic oil treatment efficaciously abrogates alcoholic steatosis and CYP2E1 induction in rat liver with restoration of AMPK activity. Chem Biol Interact. 2007; 169:80-90.
26. Gowans GJ, Hawley SA, Ross FA, Hardie DG. AMP is a true physiological regulator of AMP-activated protein kinase by both allosteric activation and enhancing net phosphorylation. Cell Metab. 2013; 18:556-566.
27. Bruckbauer A, Zemel MB, Thorpe T, Akula MR, Stuckey AC, Osborne D, Martin EB, Kennel S, Wall JS. Synergistic effects of leucine and resveratrol on insulin sensitivity and fat metabolism in adipocytes and mice. Nutr Metab (Lond). 2012; 9:77.
28. Murgas Torrazza R, Suryawan A, Gazzaneo MC, Orellana RA, Frank JW, Nguyen HV, Fiorotto ML, El-Kadi S, Davis TA. Leucine supplementation of a low-protein meal increases skeletal muscle and visceral tissue protein synthesis in neonatal pigs by stimulating mTOR-dependent translation initiation. J Nutr. 2010; 140:2145-2152.

(Received April 19, 2019; Revised May 28, 2019; Accepted June 9, 2019)